

Liver lobe-specific hydrodynamic gene delivery to baboons: A preclinical trial for hemophilia gene therapy

Kenya Kamimura,^{1,2} Tsutomu Kanefuji,¹ Takeshi Suda,³ Takeshi Yokoo,¹ Guisheng Zhang,⁴ Yutaka Aoyagi,¹ and Dexi Liu⁴

¹Division of Gastroenterology and Hepatology, Graduate School of Medical and Dental Sciences, Niigata University, Niigata, Niigata 951-8510, Japan; ²Department of General Medicine, Niigata University School of Medicine, Niigata, Niigata 951-8510, Japan; ³Department of Gastroenterology and Hepatology, Uonuma Institute of Community Medicine, Niigata University Medical and Dental Hospital, Minami Uonuma, Niigata 949-7302, Japan; ⁴Department of Pharmaceutical and Biomedical Sciences, College of Pharmacy, University of Georgia, Athens, GA 30602, USA

Hydrodynamics-based gene transfer has been successfully employed for *in vivo* gene delivery to the liver of small animals by tail vein injection and of large animals using a computer-assisted and image-guided protocol. In an effort to develop a hydrodynamic gene delivery procedure clinically applicable for gene therapy, we have evaluated the safety and effectiveness of a lobe-specific hydrodynamic delivery procedure for hepatic gene delivery in baboons. Reporter plasmid was used to assess the gene delivery efficiency of the lobe-specific hydrodynamic gene delivery, and plasmid-carrying human factor IX gene was used to examine the pattern of long-term gene expression. The results demonstrated liver lobe-specific gene delivery, therapeutic levels of human factor IX gene expression lasting for >100 days, and the efficacy of repeated hydrodynamic gene delivery into the same liver lobes. Other than a transient increase in blood concentration of liver enzymes right after the injection, no significant adverse events were observed in animals during the study period. The results obtained from this first non-human primate study support the clinical applicability of the procedure for lobe-specific hydrodynamic gene delivery to liver.

INTRODUCTION

Recent successes in gene therapy research¹⁻³ inspire new efforts to develop safer and more therapeutically effective gene therapy procedures for disease treatment. Various strategies including viral vectors,⁴ non-viral vectors,⁵ and their combination with genome editing technologies^{6,7} have been tested for this purpose. Among the non-viral strategies, hydrodynamic gene delivery is one of the promising methods that was firstly reported in 1999 by Liu et al.⁸ and Zhang et al.⁹ Hydrodynamic gene delivery employs a physical force generated by the combined effect of injection speed and volume of gene-containing solution that permeabilizes cell membrane and accomplishes intracellular gene transfer. Based on the results of gene expression studies performed in rodents, there have been attempts to use this technique for therapeutic gene transfer in the clinic. To

develop a reliable and safe procedure, the original procedure of tail vein injection was modified to target specific organs and deliver genes by employing X-ray image-guided catheterization to specific vessels¹⁰⁻¹³ and transient occlusion of blood flow to generate hydrodynamic pressure.¹⁴⁻¹⁶ In addition, we have established a computer-assisted injection device to ensure reproducibility and gene delivery efficiency with minimal volume of DNA solution.¹⁷ The safety and efficacy of the computer-controlled and image-guided hydrodynamic gene delivery were demonstrated by achieving high levels of liver lobe-specific reporter gene expression in pigs^{10,12} and dogs¹³ with a 90% reduction in injection volume per body weight from the original protocol. To further explore the applications of this procedure, this study was undertaken to perform the first preclinical trial of hydrodynamic gene delivery in baboons. The goal of the study was to evaluate the efficiency and safety of the procedure in a non-human primate animal model. For this purpose, we conducted computer-controlled, image-guided, liver lobe-specific hydrodynamic gene delivery of plasmids that express luciferase reporter and human factor IX (hFIX) in baboons.

RESULTS

Lobe-specific gene delivery and its expression in the liver of the baboon by hydrodynamic gene delivery

The image-guided, liver lobe-specific gene delivery was examined for its reliability and safety in the baboon. The procedure involves the insertion of a balloon catheter into a target hepatic vein under X-ray image guidance, balloon inflation to block the backflow

Received 20 January 2023; accepted 10 May 2023;
<https://doi.org/10.1016/j.omtn.2023.05.018>

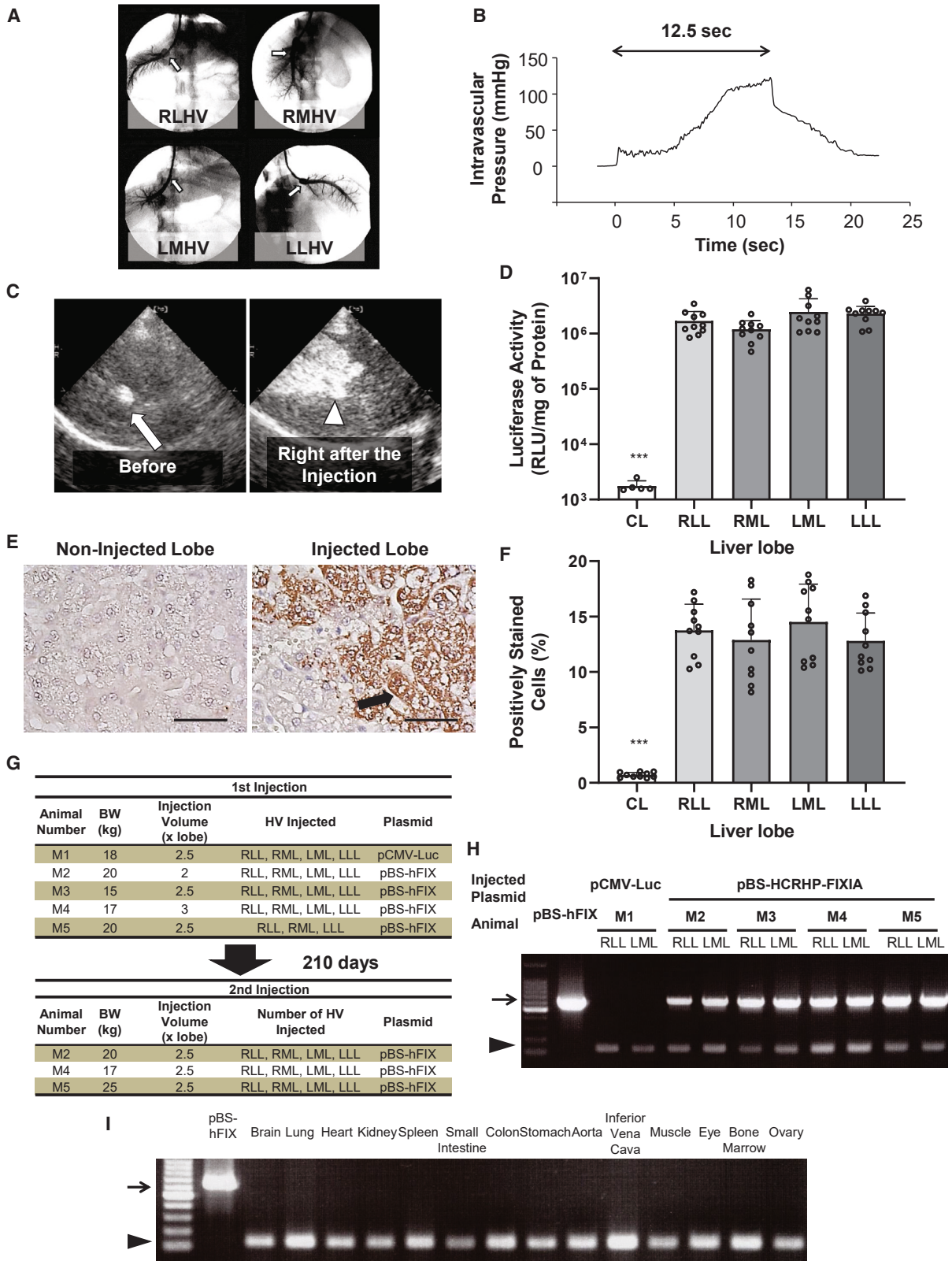
Correspondence: Kenya Kamimura, Department of General Medicine, Niigata University School of Medicine, 1-757 Asahimachi-dori, Chuo-ku, Niigata 951-8510, Japan.

E-mail: kenya-k@med.niigata-u.ac.jp

Correspondence: Dexi Liu, Department of Pharmaceutical and Biomedical Sciences, University of Georgia, College of Pharmacy, 450 Pharmacy South, Athens, GA 30602, USA.

E-mail: dliu@uga.edu





(legend on next page)

(Figure 1A), and then computer-controlled hydrodynamic injection of the pCMV-Luc plasmid DNA solution. This procedure was performed sequentially in the four hepatic veins to target the right lateral lobe (RLL), the right medial lobe (RML), the left medial lobe (LML), and the left lateral lobe (LLL) with the optimal injection volume of $2.5 \times$ lobe volume (approximately 250 mL). Using the computer-controlled injector,¹⁷ the injection time-intravascular pressure curve, which we developed in the previous study,¹² was utilized to monitor the procedure in all injections (Figure 1B). The successful lobe-specific distribution of plasmid solution was confirmed using ultrasonography upon the injection in a real-time manner (Figure 1C). The lobe-specific gene expression of luciferase was confirmed by the luciferase activity showing the highest level at 10^6 – 10^7 RLU/mg of protein in the four injected lobes homogeneously, which was significantly higher than the activity in the non-injected caudate lobe (CL) ($p < 0.001$) (Figure 1D). Immunohistochemical staining showed lobe-specific distribution of 10%–15% of positively stained cells (Figure 1E), which was significantly higher than the level in the non-injected CL ($p < 0.001$) (Figure 1F). Based on these results, the hFIX-expressing plasmid (pBS-HCRHP-FIXIA) was hydrodynamically injected with different injection volumes and numbers of hepatic veins to examine the effects of different parameters on hFIX level in the blood of the baboons (Figure 1G, 1st injection).

The lobe-specific distribution of the plasmid DNA was confirmed by polymerase chain reaction analyses of DNA isolated from the liver lobes and other organs 210 days after the first injection of M3 and 210 days after the second injection of M2, M4, and M5 baboons, respectively (Figures 1H and 1I). Extrahepatic gene transfer was not detected in the brains, lungs, hearts, kidneys, spleens, small intestines, colons, stomachs, aortas, inferior vena cava, muscles, eyes, bone marrows, and ovaries (representative data of M5 are shown in Figure 1I).

To confirm that the lack of detection of pBS-HCRHP-FIXIA in non-hepatic organs is not due to variability in DNA extraction efficiency among different tissue samples by the Qiagen DNA isolation kit, we selected three organs from the M1 baboon, the liver that showed the detectable level of transgene and kidney and lungs that showed negative signal and spiked to the same amount of tissue samples with 0, 0.1, 1.0, 10.0, or 100.0 pg of pBS-HCRHP-FIXIA plasmid, followed by polymerase chain reaction (PCR) analysis on the extracted DNA. The results show the same pattern of PCR bands among the three different tissues that were spiked with different amounts of plasmid DNA (Figure S1). These results provide evidence in support that the lack of detection among the non-hepatic tissues is likely due to lack of successful gene delivery to these organs.

Efficacy of the procedure on gene expression and effect of gene readministration

The effect of the procedure on gene expression was assessed using an hFIX-expressing plasmid (pBS-HCRHP-FIXIA) to determine the clinical applicability of the procedure in terms of the plasma level of transgene product and the feasibility of gene readministration. The first delivery of the hFIX gene was performed with a range of parameters into four baboons M2–M5 (Figure 1G) and determined the best setting that achieved the highest level of hFIX protein in the plasma. The plasmid solutions of $2 \times$, $2.5 \times$, and $3 \times$ lobe volumes were injected into each of the four hepatic veins in M2, M3, and M4, respectively, and the coagulation activity and plasma concentration of hFIX were evaluated. Based on the results of our previous study, an injection speed of 20 mL/s was used.¹³ For M5, the plasmid solution was injected through three hepatic veins with $2.5 \times$ lobe volume to assess the reduction effect for the number of targeting hepatic veins (Figure 1G). Among the three baboons M2–M4, M3 showed the highest plasma hFIX level of 31.4 μ g/mL (Figure 2A) along with the

Figure 1. Liver lobe-specific hydrodynamic gene delivery in baboons

(A) Fluoroscopic images of hepatic veins following the lobe-specific catheterization in baboon liver. RLHV, right lateral hepatic vein; RMHV, right medial hepatic vein; LMHV, left medial hepatic vein; LLHV, left lateral hepatic vein. The white arrows indicate the balloon inflated. (B) Intravascular pressure profile upon injection of $2.5 \times$ lobe volume of DNA solution in 12.5 sec. (C) Ultrasonographic images before and after lobe-specific hydrodynamic injection into the RMHV. The injected DNA solution in the target RMHV was revealed by ultrasound upon injection. The white arrow indicates the balloon at the tip of the catheter. The white arrowhead indicates the distribution of the injected solution. (D) Average level of luciferase gene expression 24 h after hydrodynamic gene delivery in each liver lobe in baboon M1 (CL, caudate lobe; RLL, right lateral lobe; RML, right medial lobe; LML, left medial lobe; LLL, left lateral lobe). $n = 10$ each for the RLL, RML, LML, and LLL, $n = 5$ for the CL. The values represent mean \pm SD. *** $p < 0.001$ between all injected lobes and CL. One-way ANOVA was followed by Bonferroni's multiple comparison test. (E) Representative images of immunohistochemical staining of liver sections using anti-luciferase antibody. The black arrow indicates positively stained hepatocytes. Scale bars represent 50 μ m. (F) A quantitative analysis of percentage of positively stained cells. 10 liver samples randomly collected from each lobe (a total of 50 samples in a liver) in M1 were immunohistochemically stained with anti-luciferase antibody, and quantitative analysis was performed on two fields (a total of 50 fields in a liver) from each section using the ImageJ software (version 1.54d; National Institutes of Health, USA). The values represent mean \pm SD. *** $p < 0.001$ between all injected lobes and CL. One-way ANOVA was followed by Bonferroni's multiple comparison test. RLL, right lateral lobe; RML, right medial lobe; LML, left medial lobe; LLL, left lateral lobe; CL, caudate lobe. (G) Parameters considered for hydrodynamic injections in each baboon. Body weight, injection volume, hepatic vein targeted, and injected plasmid are shown. (H) Multiplex PCR analysis of plasmid distribution among different liver lobes. DNA extracted from baboon livers was used as template for 30 cycles of PCR amplification using the forward primer for the hAAT promoter sequence and the reverse primer for the hFIX intron in pBS-HCRHP-FIXIA plasmid. The glyceraldehyde 3-phosphate dehydrogenase gene (*Gapdh*) gene was used as an internal control. Lanes are as follows: 1, 10 ng/mL of pBS-HCRHP-FIXIA plasmid DNA; 2, 4, 6, 8, and 10, RLL from M1–M5, respectively; 3, 5, 7, 9, and 11, LML from M1–M5, respectively. The black arrow represents the 647-bp pBS-HCRHP-FIXIA plasmid fragment. The black arrowhead represents the 122-bp *Gapdh* fragment. (I) Tissue distribution of plasmid DNA. Multiplex PCR analysis was performed on total DNA extracted from various organs in M5 using 30 cycles of PCR amplification with a forward primer for the hAAT promoter sequence and the reverse primer for the hFIX intron in pBS-HCRHP-FIXIA plasmid. Glyceraldehyde 3-phosphate dehydrogenase gene (*Gapdh*) gene was used as internal control. Lanes are as follows: 1, 10 ng/mL of pBS-HCRHP-FIXIA plasmid DNA; 2, brain; 3, lung; 4, heart; 5, kidney; 6, spleen; 7, small intestine; 8, colon; 9, stomach; 10, aorta; 11, inferior vena cava; 12, muscle; 13, eye; 14, bone marrow; 15, ovary. The black arrow represents the 647-bp pBS-HCRHP-FIXIA plasmid fragment. The black arrowhead represents the 122-bp *Gapdh* fragment.

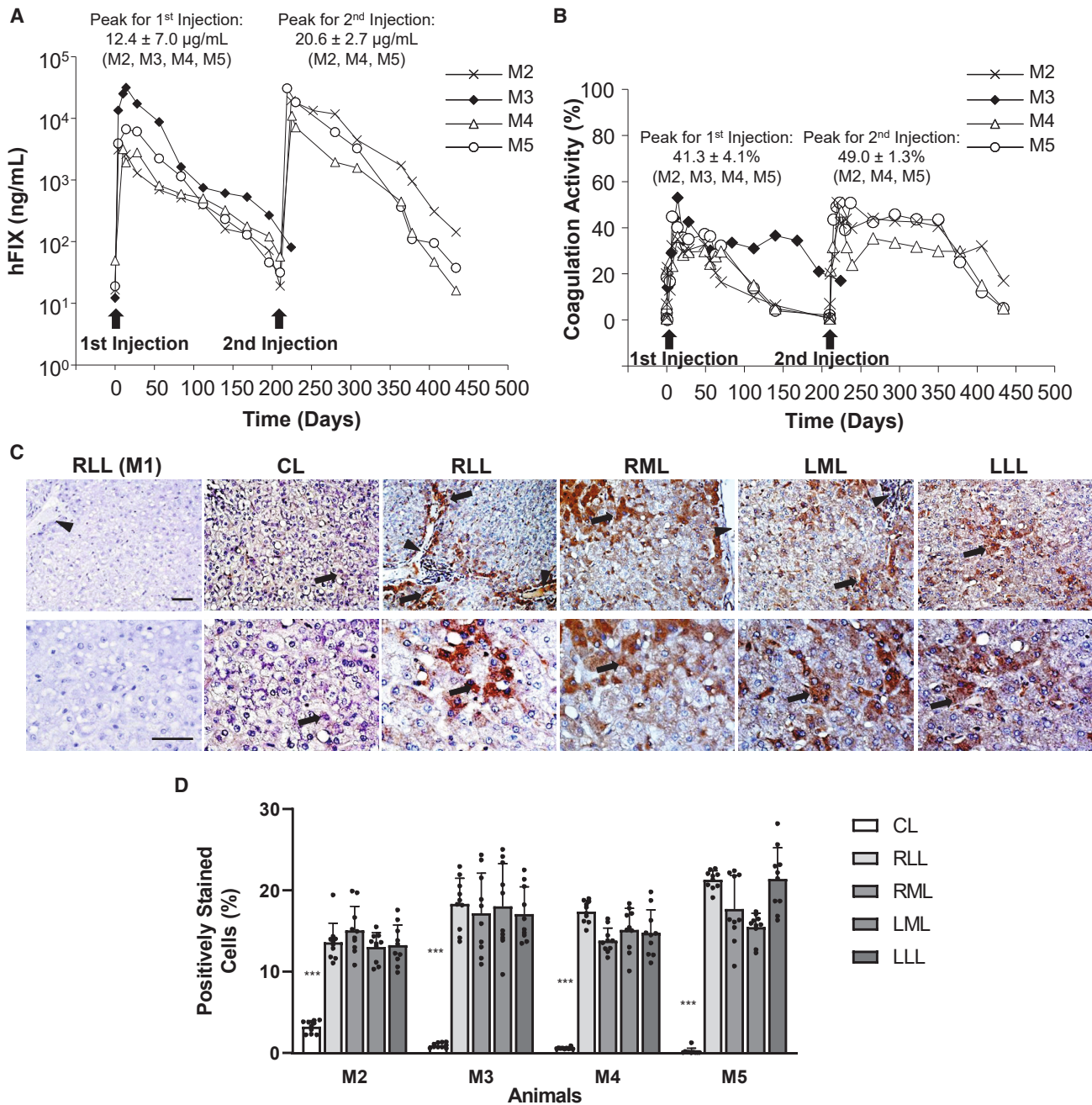


Figure 2. Efficacy of the lobe-specific hydrodynamic delivery on gene expression and effect of gene readministration

(A and B) The plasma concentration and coagulation activity of hFIX in M2–M5 after the first and second set of sequential injections in M2, M4, and M5 baboons. Blood concentration of hFIX and coagulation activity values are expressed as mean \pm SE. (C) The representative images of immunohistochemical staining of hFIX in the RLL of M1 baboon injected with pCMV-Luc and each lobe of M3 baboon injected with pBS-HCRHP-FIXIA. Scale bar represents 50 μm . Black arrows represent positively stained hepatocytes, and black arrowheads represent central hepatic vein. (D) A quantitative analysis of the percentage of positively stained cells with anti-hFIX antibody. The values represent mean \pm SD. *** $p < 0.001$ between all injected lobes and CL. One-way ANOVA followed by Bonferroni's multiple comparison test. CL, caudate lobe; RLL, right lateral lobe; RML, right medial lobe; LML, left medial lobe; LLL, left lateral lobe.

coagulation activity of 53% 10 days after the gene delivery, which was sustained above the therapeutic level of approximately 30% for the subsequent 200 days (Figure 2B). On the contrary, baboons M2 and

M4 showed peak levels of 2.6 and 3.2 $\mu\text{g/mL}$, which were approximately 10 times lower than the concentration in M3 and slowly declined with time and returned to the background value (Figure 2A).

Coagulation activities, which peaked at up to 35% and 36%, slowly declined over the course and returned to background level by 100 days following the first injection (Figure 2B). In M5, the highest hFIX concentration and coagulation activity values were 6.6 $\mu\text{g/mL}$ and 45%, respectively, which were higher than the values for M2 and M4 but substantially lower than those for M3. There was no increase in hFIX protein or coagulation activity after the delivery of pCMV-Luc plasmids (data not shown). These results suggest that the lobe-specific hydrodynamic gene delivery injecting $2.5\times$ lobe volume into four hepatic veins is a better condition for delivering hFIX-expressing plasmid to achieve the suprathysiologic level of hFIX in non-human primates. To confirm the efficacy of the tested parameters ($2.5\times$ lobe volume into four hepatic veins) and evaluate the safety of readministration, M2, M4, and M5 received a second injection of pBS-HCRHP-FIXIA plasmids under the tested conditions 210 days after the first injection when both the plasma hFIX level and the coagulation activity returned to the background levels. The hFIX expression in the plasma peaked at 19.3, 12.0, and 30.5 $\mu\text{g/mL}$ in M2, M4, and M5, respectively, within 10 days after the second injection, which was 5–10 times higher than the level obtained after the first injection (Figure 2A). The level was maintained at >1.0 $\mu\text{g/mL}$ for 100–150 days. Consistently, coagulation activities achieved 51%, 49%, and 47%, respectively, which were approximately 20% higher than those after the first injection (Figure 2B) and were similar to that in M3. To confirm the site-specific gene expression in the liver, all animals were euthanized 210 days after injection with $2.5\times$ lobe volume into four hepatic veins (after the first injection to M3 and the second injection to M2, M4, and M5). Immunohistochemical staining of liver tissues using anti-hFIX antibody showed lobe-specific distribution of the positively stained cells compared with the non-injected CL (Figure 2C), and the proportion of positively stained cells ranged from 15% to 25% of the hepatocytes in the injected liver lobes with no significant difference among animals and lobes (Figure 2D). The positively stained cells were enriched in the area close to the central hepatic vein, zone III (Figure 2C). The LML in M5, which received the injection only once, showed a relatively lower number of positively stained cells in comparison with other lobes in the same animal. These results suggest the reproducibility of the procedure with optimal parameters and the consistent gene expression upon sequential administration in baboons. Overall, these results support the notion that computer-controlled image-guided hydrodynamic gene delivery is capable of achieving physiologic levels of gene expression.

Safety evaluation

To determine the safety of the procedure, biophysical and biochemical analyses were performed on the baboons during and after the gene delivery. All four baboons of M2–M5 showed no body weight loss after hydrodynamic injection of the hFIX-expressing plasmid (Figure 3A). Other than a transient increase in carbon dioxide concentration in the expiratory air, no significant changes in heart rate, blood oxygen saturation, or body temperature were observed after the sequential hydrodynamic injections of $2.5\times$ lobe volume DNA solution, including either pCMV-Luc or pBS-HCRHP-FIXIA, into four hepatic veins of M1–M4 (Figure 3B). No changes were seen on the

electrocardiogram before, immediately after, and 5 and 20 min after the injection (Figure 3C). The serum levels of liver-related enzymes showed 10- to 20-fold increase in aspartate aminotransferase (AST) and alanine aminotransferase (ALT) 24 h after each injection of $2.5\times$ lobe volume in M2–M5, which returned to normal within a week (Figure 3D). In terms of lactate dehydrogenase (LDH), the serum concentration increased 2- to 3-fold 24 h after each round of injection and remained elevated for 200 days (Figure 3D). Hematoxylin and eosin staining was used to evaluate the impact of hydrodynamic injection on liver tissues 24 h after the injection in M1. The sinusoid and hepatocytes were significantly larger in the injected lobes than the non-injected CL, and the cytoplasm of the hepatocytes was more transparent (Figure 3E). No differences were observed in the lobes of the M3 baboon 210 days after the second injection of pBS-HCRHP-FIXIA (Figure 3F). No inflammatory cell infiltration or liver fibrosis that indicates chronic damage was seen in any of M2–M5 on 210 days after $2.5\times$ lobe volume hydrodynamic injection (data not shown). To further examine the safety of the procedure, time-dependent changes in immune-related cytokines were assessed after hydrodynamic gene delivery (Figure 4). There were no significant increases in the serum concentration of interferon- γ , interleukin-2, and interleukin-8 even after the second injection of the hFIX-expressing plasmid, while a transient increase was observed for muscle stretching-related cytokines of tumor necrosis factor alpha (TNF- α), monocyte chemoattractant protein-1 (MCP-1), and interleukin-6 (IL-6) 2 h after the injection (Figure 4).

DISCUSSION

While we have previously demonstrated the efficacy of the lobe-specific hydrodynamic delivery of reporter genes to the liver in large animals,^{10,12,13} the level of gene expression achieved at therapeutic level has not been reported. Regarding hemophilia gene therapy, various gene delivery methods, including viral vector-based,^{18–22} non-viral vector-based,^{23,24} and *in vivo* gene editing procedures,^{25–29} have been studied in small animal models, but the efficacy in large animal models was insufficient.^{20,22,30} In this study, we demonstrate that the appropriate hydrodynamic parameters, including injection volumes and speed, achieved the therapeutic level of hFIX in baboons. In addition, gene expression at therapeutic level was regained from the baseline with the repeated administration 210 days after the first injection. We also demonstrate in baboons that the image-guided and liver lobe-specific hydrodynamic gene delivery of hFIX-expressing plasmid achieved site-specific gene delivery and coagulation activity above the therapeutic threshold of 10%³¹ and plasma concentration of hFIX greater than 1.0 $\mu\text{g/mL}$ for 100–150 days with no persistent negative events.

Hemophilia gene therapy has been conducted using adeno-associated virus (AAV) vectors.^{18,32,33} It has been previously reported that AAV system is capable of successful gene delivery and induction of coagulation activity above the therapeutic threshold. The drawback of the AAV system revealed in these earlier studies, however, is the immunologic responses elicited by preexisting anti-AAV neutralizing antibodies,³⁴ innate and adaptive immune response to the viral vector, and cytotoxic T cell responses against the vector

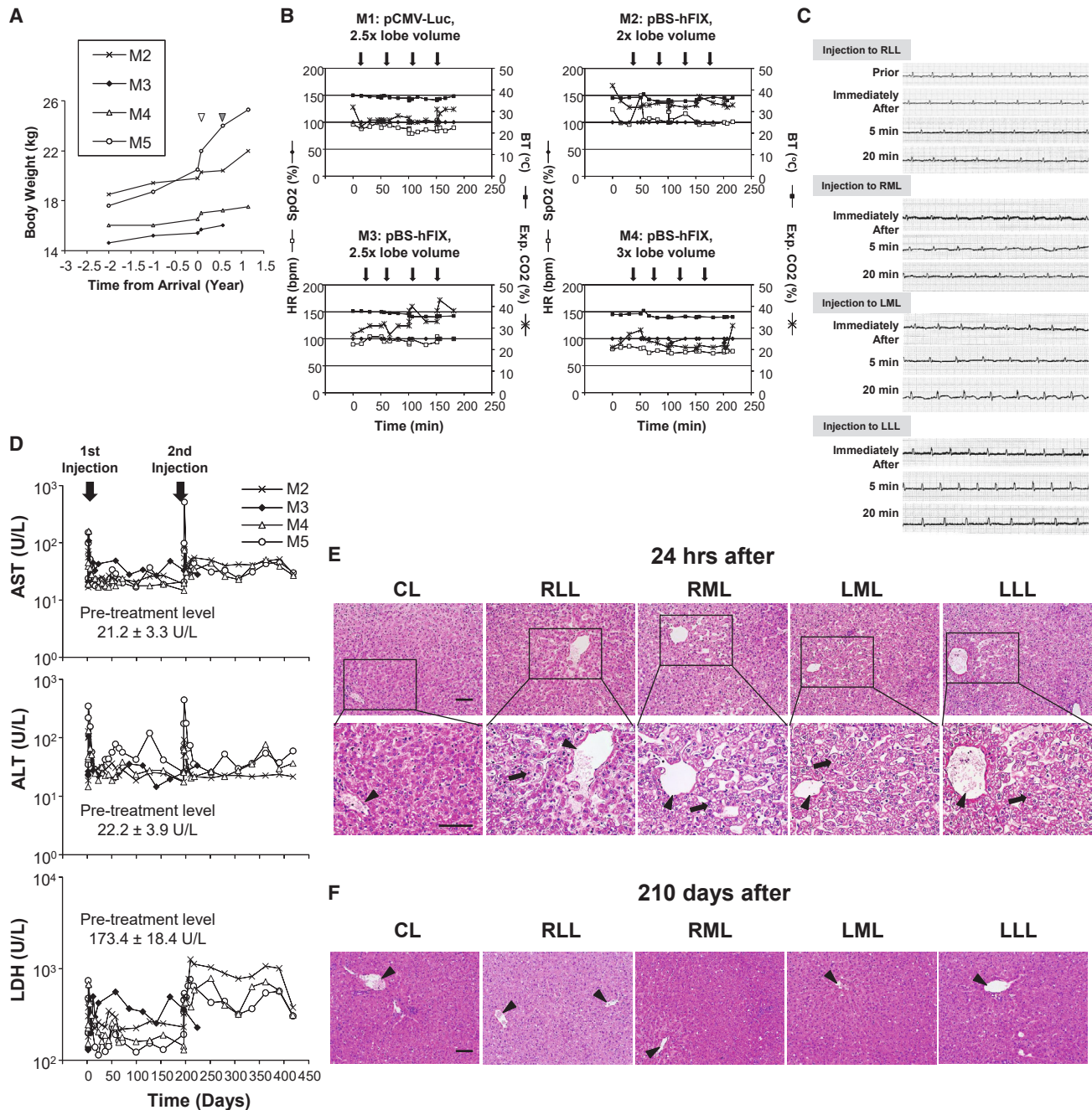
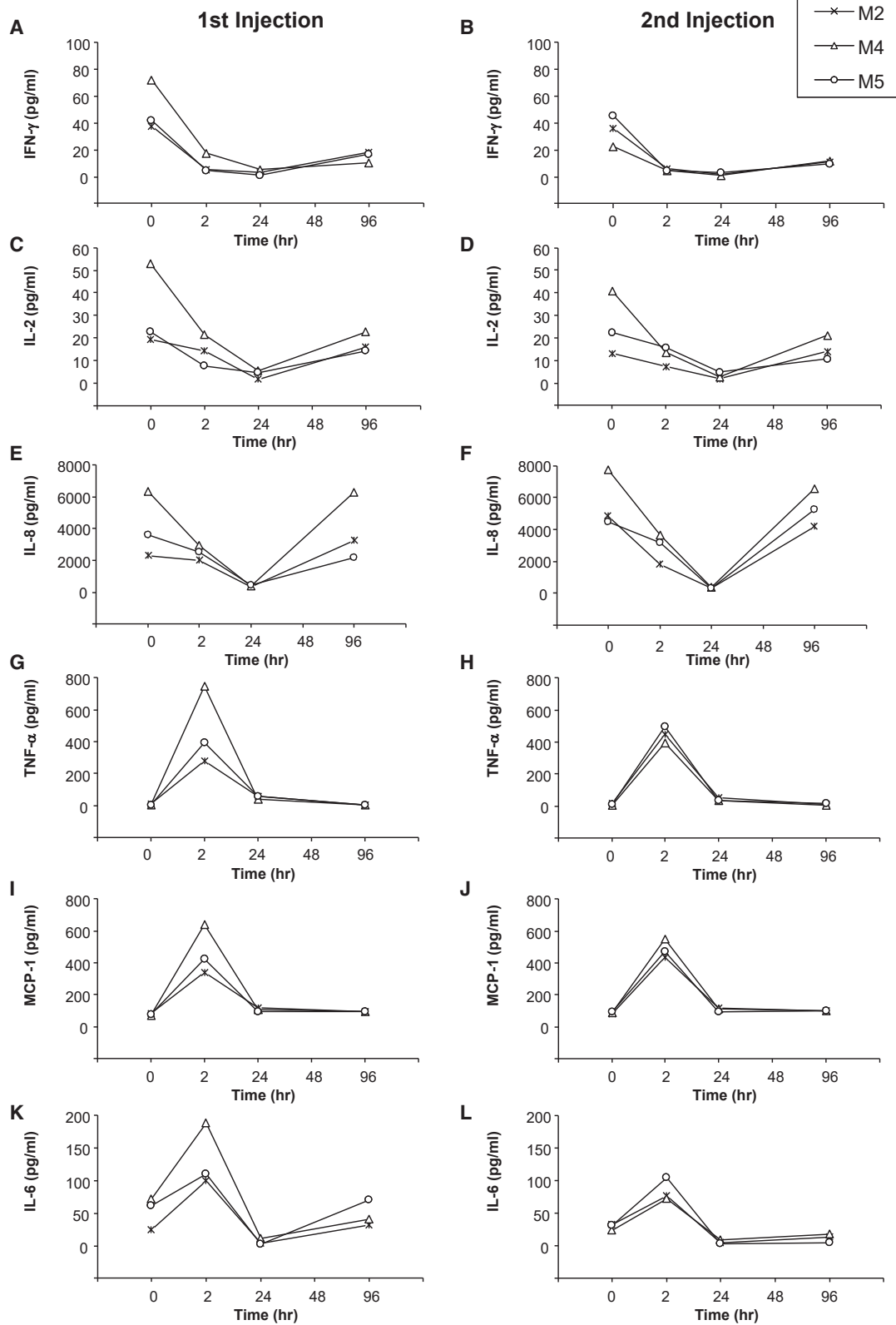


Figure 3. Safety assessment

(A) Body weights of the baboons before and after hydrodynamic gene delivery. White and black arrowheads indicate the first and second set of injections on day 0 and 210. (B) Biophysical assessment of heart rate, blood oxygen saturation (SpO₂), body temperature, and carbon dioxide concentration in expiratory air (Exp. CO₂) upon the hydrodynamic gene delivery in M1–M4 with various injection parameters. Black arrows indicate the injections to RLL, RML, LML, and LLL. (C) Changes in electrocardiogram during the sequential injections into four liver lobes of RLL, RML, LML, and LLL in M3. (D) Blood concentrations of aspartate aminotransferase (AST), alanine aminotransferase (ALT), and lactate dehydrogenase (LDH). Black arrows indicate the first and second set of injections on day 0 and 210. Blood samples were collected from the cephalic vein of M2–M5 before (time = 0), 1, 2, and 24 h, and 4, 7, 14, 28, 56, 84, 112, 140, 168, 196, and 210 days after the first set of hydrodynamic injections, and additionally from M2, M4, and M5 at the same time points after the second set of hydrodynamic injections. Pre-treatment levels of AST, ALT, and LDH are presented as mean \pm SE. (E) Tissue damage was evaluated by hematoxylin and eosin staining of the liver samples from each lobe of M1 baboon 24 h after the injection of pCMV-Luc plasmid DNA and (F) from M3 baboon 210 days after the second set of injections of pBS-HCRHP-FIXIA plasmid DNA. Scale bars represent 100 μ m. Black arrow indicates the hepatocyte with increased transparency, and black arrowheads represent central hepatic vein. CL, caudate lobe; RLL, right lateral lobe; RML, right medial lobe; LML, left medial lobe; and LLL, left lateral lobe.



(legend on next page)

capsid protein^{35,36} hampering persistent transgene expression and precluding repetitive administration.^{24,37,38} Comparing to AAV system, hydrodynamic delivery of naked DNA elicited only a minor immunological response, and therefore, it is possible to regain the therapeutic level of gene expression via repeated administration after the transgene express had returned to a basal level. In addition, it was reported that AAV vector administration resulted in the integration of the AAV genome, leading to the clonal expansion of transduced liver cells in dogs³⁰ and the development of liver cancer in 33% of the mice treated.³⁹ At this point, it is reasonable to assume that hydrodynamic delivery of plasmid DNA without any other component involved poses the least possibility of causing an integration event in the host genome.

The fact that the image-guided, liver lobe-specific gene delivery revealed considerably low gene expression in non-injected CL and non-injected organs adds to our method's targeting specificity and long-term biological safety. The impact of the hydrodynamic injection is generated by the combined effects of injection volume and speed,^{8,40,41} which resulted in rapid liver expansion, stretching of the hepatocytes, and increase of hepatocyte cell membrane permeability, allowing gene-containing solution to enter cell interior. Tissue enlargement and increased transparency of the hepatocyte cytoplasm revealed by histological examination coincide with the release of cytoplasmic AST, ALT, and LDH into the blood.^{10,12,13} As previously reported in mice,^{8,40} pigs,¹² and dogs,¹³ these changes were related to successful gene delivery and the induction of the cytokines related to myocytes and vascular stretching after hydrodynamic delivery, such as TNF- α ,⁴² MCP-1,^{43,44} and IL-6.⁴² In this context, it is interesting to observe a sustained elevation of LDH indicating the presence of tissue damage. While additional work is needed to sort out where the damage occurs, the transient nature of rising blood concentration of liver-specific enzymes such as AST and ALT induced by the procedure would suggest that the LDH release may not involve hepatocytes. However, as the time course of LDH resembled with that of coagulation activity, it is also possible that excessive expression of hFIX in liver cells may change the anaerobic metabolic conditions in the cells.⁴⁵ Additional analysis concentrating on the LDH isozymes and longer-term studies will illustrate the mechanisms further. A transient increase in carbon dioxide concentration in the expiratory air upon the injection could be caused by the high-pressure carbon dioxide used by the in-house-developed hydrodynamic injector to drive the DNA solution into the hepatic veins.¹⁷ To overcome this problem, we have been developing a new injection device using an electric motor to drive the pressurized injection.²³

Lack of transgene detected in the non-hepatic organs (Figure 1I) supports the notion that the hydrodynamic impact, essential for intracellular gene transfer, is not established in the non-hepatic tissues following the procedure of our lobe-specific hydrodynamic injection.

However, it is important to point out that lack of reporter gene detected in the non-hepatic tissues demonstrated by PCR is an important piece of evidence in support of liver-specific gene delivery of the procedure. This conclusion derived from the results in Figure 1I is based on a pre-assumption that Qiagen kit employed for DNA extraction has equal efficiency in extracting plasmid DNA from all of the tissues of the organs examined, although this assumption has been partially validated in the liver, kidney, and lung (Figure S1).

The level and persistency of gene expression have been the major focus of gene therapy. The blood concentration of hFIX in baboons receiving hydrodynamic delivery of hFIX gene is greater than 1.0 $\mu\text{g}/\text{mL}$ for 100–150 days, reaching a similar level obtained in the rats with $>1.0 \mu\text{g}/\text{mL}$ lasting for 70 days.²⁴ However, this time frame is significantly shorter than >5 years achieved by the AAV vectors in rhesus macaques.^{20,21} Gradual decrease of hFIX level seen in our study is likely caused by gene silencing, although production of the anti-hFIX inhibitors remains another possibility. A similar profile of hFIX level in blood between the first and second hydrodynamic gene delivery does not support the possibility of generation of anti-hFIX antibodies in baboons. It remains to be seen in non-human primates whether the strategies proven effective in small animals using immune suppression agents, transposon systems, the minicircle plasmid DNA, and even a CRISPR-Cas9-based genome editing system will sustain the transgene expression for a desirable time period for effective gene therapy.

In summary, the following are the major findings of our work: (1) the site-specific gene delivery and transgene expression were achieved safely and effectively in the baboons, (2) no immunological reactions were observed even after the second injection of the same genes, and (3) the hydrodynamic parameters employed are effective but not optimal and need more testing with a larger number of animals for improved delivery efficiency and safety. More importantly, our results, although involving only five baboons, provide direct evidence in support the notion that lobe-specific hydrodynamic gene delivery to liver is applicable to humans, and clinical trials can be conducted.

MATERIALS AND METHODS

Materials

The pCMV-Luc plasmid containing firefly luciferase cDNA driven by a CMV promoter and pBS-HCRHP-FIXIA were purified by CsCl-ethidium bromide gradient centrifugation and kept in a Tris-EDTA buffer. The pBS-HCRHP-FIXIA was kindly provided by Dr. Carol Miao. The pBS-HCRHP-FIXIA is abbreviated from pBS-ApoEHCR-hAATp-hFIX+IntA-bpA, and the expression cassette contains a human $\alpha 1$ anti-trypsin (hAAT) promoter, hFIX cDNA, a truncated hFIX intron A, and a bovine growth hormone polyadenylation signal.^{46–48} The purity of the plasmid preparation was determined by measuring absorbance at 260 and 280 nm and 1% agarose gel electrophoresis.

Figure 4. Effect of the procedure and readministration of plasmid DNA on immune- and muscle stretching-related cytokines

Blood samples were collected from the cephalic vein of M2, M4, and M5 before (time = 0), 2, 24, 48, and 96 h after the first and second set of hydrodynamic injections. Concentrations of interferon- γ (IFN- γ) (A, B), interleukin-2 (IL-2) (C, D), interleukin-8 (IL-8) (E, F), tumor necrosis factor alpha (TNF- α) (G, H), monocyte chemoattractant protein-1 (MCP-1) (I, J), and interleukin-6 (IL-6) (K, L).

The luciferase assay kit was obtained from Promega (Madison, WI, USA). The introducer and the 9-Fr sheath for image-guided catheter insertion were obtained from COOK (Bloomington, IN, USA), and the guide wire (ZIP wire) was obtained from Boston Scientific (Natick, MA, USA). Injection balloon catheters (9 Fr) were purchased from Tokai Medical (Kasugai, Aichi, Japan). The MIKRO TIP catheter transducer was obtained from Millar (Houston, TX, USA). The contrast medium (OXILAN) was purchased from Guerbet (Bloomington, IN, USA). The WavelineVet Vital Signs Monitor to monitor physiological parameters in animals was obtained from DRE Veterinary (Louisville, KY, USA).

Animal experiments

Five female baboons (15–20 kg) were purchased from the University of Oklahoma and named M1–M5 (Figure 1G). All animal experiments were conducted in full compliance with the regulation of and approval by the Institutional Animal Care and Use Committee of the University of Pittsburgh, Pittsburgh, Pennsylvania, which also approved the study protocol (0909604). All animals received humane care according to the criteria outlined in the “Guide for the Care and Use of Laboratory Animals” prepared by the National Academy of Sciences (USA). Throughout the study, the animals were monitored for general condition and body weight, as well as their electrocardiogram, heart rate, blood oxygen saturation, body temperature, and carbon dioxide concentration in the expiratory air during the gene delivery procedure. Through a skin incision on the baboons, a 9-Fr short sheath was inserted in the jugular vein under general anesthesia. The animals were then placed on the YSF-100 fluoroscopy machine table (Shimadzu, Nakagyo-ku, Kyoto, Japan). Following an insertion of the injection catheter, the balloon was inflated by injection of 1 mL of phase contrast medium. Obstruction of blood flow was verified by injecting a small volume of phase contrast medium into the vasculature through the catheter.

Hydrodynamic injection

Injections of saline containing either pCMV-Luc (100 µg/mL) or pBS-HCRHP-FIXIA plasmid DNA (100 µg/mL) via the balloon catheter were performed with the injection speed of 20 mL/s using the *Hydrojector* according to data obtained in the previous studies.^{10,12,13} The injection volume was determined based on the estimated lobe volume using the method of previous studies.^{12,49} Liver lobe-specific hydrodynamic gene delivery was performed for five baboons on day 1 (Figure 1). Three of these baboons (M2, M4, and M5) received a second injection 210 days after the first injection. Intravascular pressure was transmitted to the computer using a MIKRO TIP catheter transducer inserted via the catheter into the hepatic veins. After the injection, the balloon remained inflated for 20 min and then slowly deflated. Sequential injection into multiple hepatic veins was performed with 30-min intervals between injections. The animals other than M1 received an antibiotic with amoxicillin for 5 days after hydrodynamic gene delivery.

Analysis of luciferase gene expression

The liver of M1 was removed 24 h after hydrodynamic delivery of the pCMV-Luc plasmid. 10 liver samples from each of the four injected

lobes and five samples from the non-injected CL were collected for the luciferase assay. Luciferase and protein assays were performed according to the previously established procedure.⁸ 10 liver samples were collected from each of the five lobes and fixed in 10% formalin, embedded in paraffin, and sections (10 µm) were prepared. Standard immunohistochemical staining was performed with a goat anti-luciferase polyclonal antibody (G7451, 1:50 dilution; Promega, Madison, WI), VECTASTAIN Elite ABC Goat IgG kit (PK-6105; Vector Laboratories, Burlingame, CA) and DAB chromogen tablet (Muto Pure Chemicals, Bunkyo-ku, Tokyo) for luciferase staining. A microscopic examination was performed, and photo images were recorded using a Leitz DMRB imaging system (Leica, Wetzlar, Germany).

Analysis of serum hFIX expression

M2–M5 were hydrodynamically injected with the pBS-HCRHP-FIXIA plasmid. Blood samples were collected from their cephalic veins before and 4, 7, 14, 28, 56, 84, 112, 140, 168, 196, and 210 days after the first and second gene delivery of pBS-HCRHP-FIXIA plasmid. Plasma samples were collected for the enzyme-linked immunosorbent assay (ELISA) and assay for coagulation activity. For ELISA, a mouse anti-hFIX monoclonal antibody (clone HIX-1, F2645, Sigma, St. Louis, MO) was used for plate coating, and an HRP-conjugated goat anti-hFIX polyclonal antibody (GAFIX-HRP, Affinity Biologicals, Ancaster, ON) was used as the second antibody for binding to hFIX that bound to the well, as previously reported.⁵⁰ The coagulation activity was quantified by the clotting factor test for factor IX using factor IX-deficient plasma, which was outsourced to BML (Shibuya-ku, Tokyo, Japan).

Histological analysis for hFIX expression

Tissue samples for immunohistochemical staining were collected 210 days after the first injection of pBS-HCRHP-FIXIA for hFIX staining in M3 and 210 days after the second injection in M2, M4, and M5. Five liver sections from each of the five lobes ($n = 25$ from each animal) in four baboons (M2–M5) and two sections each from a normal baboon ($n = 10$) were immunohistochemically stained with anti-luciferase (control) or anti-hFIX antibody. Tissues were fixed in 10% formalin upon collection and embedded in paraffin. Sections (10 µm) were prepared, and standard immunohistochemistry was performed. A rabbit anti-hFIX polyclonal antibody (HPA 000254, 1:100 dilution; Sigma), VECTASTAIN Elite ABC Rabbit IgG kit (PK-6101; Vector Laboratories), and DAB chromogen tablet (Muto Pure Chemicals) were used for hFIX staining, as reported previously.²⁷ Two fields from each section (a total of 50 fields for each animal) were randomly captured for hFIX staining, and quantitative analysis of positively stained cells was performed using ImageJ software (version 1.54d; National Institutes of Health, USA) following a previously reported method.⁵¹

Genomic DNA isolation and polymerase chain reaction analysis

Sections of the livers, brains, lungs, hearts, kidneys, spleens, small intestines, colons, stomachs, aortas, inferior vena cava, muscles, eyes, bone marrows, and ovaries were collected, and DNA was isolated using a DNA extraction kit (Qiagen, Germany). Multiplex PCR was

performed on the samples, and a vector DNA with the forward PCR primer GGATCCACTGCTTAAATACG from the hAAT promoter sequence and the reverse primer GATTTCAAAGTGGTAAGTCC from the FIX intron was used to detect plasmid DNA expressing hFIX following Manno et al.³⁷ The *Gapdh* gene was used as an internal control with the forward primer AGGTCGGAGTGAACGGA TTTG and the reverse primer TGTAGACCATGTAGTGGAG GTCA. Samples of 2 μ L were amplified in a 20- μ L PCR reaction with a program of 10 min at 95°C and 30 cycles for 30 s at 95°C, 30 s at 55°C, and 1 min at 72°C, followed by a 7-min extension at 72°C. PCR products were separated on a 3% agarose gel in an electric field of 17 V/cm and stained with ethidium bromide.

Assessment of tissue damage

Blood samples were collected from the cephalic vein of M2–M5 before (time = 0), 1, 2, and 24 h, and 4, 7, 14, 28, 56, 84, 112, 140, 168, 196, and 210 days after the first hydrodynamic injection and also from M2, M4, and M5 at the same time points after the second hydrodynamic injection. Serum biochemical analyses were performed by the Cleveland Office of Marshfield Labs. The liver tissue samples collected from a normal baboon, M1 (24 h after the injection of pCMV-Luc), and M2–M5 (210 days after the second injection of pBS-HCRHP-FIXIA) were analyzed by hematoxylin and eosin staining for tissue damage. Hematoxylin and eosin staining was performed on liver tissues in the pathology laboratory of the Department of Pathology, University of Pittsburgh. The cytokines were analyzed using blood samples obtained before (time = 0), 2, 24, 48, and 96 h by GeneticLab (Sapporo, Hokkaido, Japan) using the Luminex 200 System with the MILLIPLEXMAP Non-Human Primate Cytokine Magnetic Bead Panel kit (Merck Millipore, PRCYTOMAG-40K-08).⁵²

Statistical analysis

The luciferase and hFIX assays were evaluated by analysis of variance (ANOVA), followed by Bonferroni's multiple comparison test. For the analyses, GraphPad Prism 9 software (version 9.3.1; GraphPad, San Diego, CA, USA) was used, and $p < 0.05$ was considered statistically significant.

DATA AVAILABILITY

The authors confirm that the data supporting the findings of this study are available within the article.

SUPPLEMENTAL INFORMATION

Supplemental information can be found online at <https://doi.org/10.1016/j.omtn.2023.05.018>.

ACKNOWLEDGMENTS

The authors thank Michael Maranowski, Robert Wagner, Michael Nakon Jr, and all staff members in the Division of Laboratory Animal Resources at the University of Pittsburgh for their excellent assistance with animal care. The authors also thank Miss Ryan Fugett and Enago for the critical reading of the manuscript and English language review. The research in the authors' laboratory has been supported in part by grant support from the National Institutes of Health (EB002946 and

HL075542) to D.L. and from the Japanese Society for the Promotion of Sciences (22890064, 23790595, 26860354, 17K09408, 20K08379, and 23H02763), Takeda Science Foundation Grant, Takara Bio Award, and Takara Bio Research Grant from JSST, and Adaptable and Seamless Technology Transfer Program through target-driven R&D, JST to K.K.

AUTHOR CONTRIBUTIONS

K.K. and D.L. conceived and designed the experiments. K.K., T.K., T.S., T.Y., G.Z., and D.L. conducted the experiments. K.K., T.K., and T.S. performed the animal study. Y.A. conducted the data analysis. K.K. and D.L. wrote the manuscript, which was read, edited, and approved by all authors.

DECLARATION OF INTERESTS

The authors declare no competing financial interests.

REFERENCES

- Bulaklak, K., and Gersbach, C.A. (2020). The once and future gene therapy. *Nat. Commun.* *11*, 5820.
- High, K.A., and Roncarolo, M.G. (2019). Gene therapy. *N. Engl. J. Med.* *381*, 455–464.
- Dunbar, C.E., High, K.A., Joung, J.K., Kohn, D.B., Ozawa, K., and Sadelain, M. (2018). Gene therapy comes of age. *Science* *359*, eaan4672.
- Fakhiri, J., and Grimm, D. (2021). Best of most possible worlds: hybrid gene therapy vectors based on parvoviruses and heterologous viruses. *Mol. Ther.* *29*, 3359–3382.
- Zu, H., and Gao, D. (2021). Non-viral vectors in gene therapy: recent development, challenges, and prospects. *AAPS J.* *23*, 78.
- Wang, L., Breton, C., Warzecha, C.C., Bell, P., Yan, H., He, Z., White, J., Zhu, Y., Li, M., Buza, E.L., et al. (2021). Long-term stable reduction of low-density lipoprotein in nonhuman primates following in vivo genome editing of PCSK9. *Mol. Ther.* *29*, 2019–2029.
- Ramirez-Phillips, A.C., and Liu, D. (2021). Therapeutic genome editing and in vivo delivery. *AAPS J.* *23*, 80.
- Liu, F., Song, Y., and Liu, D. (1999). Hydrodynamics-based transfection in animals by systemic administration of plasmid DNA. *Gene Ther.* *6*, 1258–1266.
- Zhang, G., Budker, V., and Wolff, J.A. (1999). High levels of foreign gene expression in hepatocytes after tail vein injections of naked plasmid DNA. *Hum. Gene Ther.* *10*, 1735–1737.
- Kamimura, K., Suda, T., Xu, W., Zhang, G., and Liu, D. (2009). Image-guided, lobe-specific hydrodynamic gene delivery to swine liver. *Mol. Ther.* *17*, 491–499.
- Kamimura, K., Zhang, G., and Liu, D. (2010). Image-guided, intravascular hydrodynamic gene delivery to skeletal muscle in pigs. *Mol. Ther.* *18*, 93–100.
- Kamimura, K., Suda, T., Zhang, G., Aoyagi, Y., and Liu, D. (2013). Parameters affecting image-guided, hydrodynamic gene delivery to swine liver. *Mol. Ther. Nucleic Acids* *2*, e128.
- Kamimura, K., Kanefuji, T., Yokoo, T., Abe, H., Suda, T., Kobayashi, Y., Zhang, G., Aoyagi, Y., and Liu, D. (2014). Safety assessment of liver-targeted hydrodynamic gene delivery in dogs. *PLoS One* *9*, e107203.
- Aliño, S.F., Herrero, M.J., Noguera, I., Dasi, F., and Sánchez, M. (2007). Pig liver gene therapy by noninvasive interventionist catheterism. *Gene Ther.* *14*, 334–343.
- Brunetti-Pierri, N., Stapleton, G.E., Law, M., Breinholt, J., Palmer, D.J., Zuo, Y., Grove, N.C., Finegold, M.J., Rice, K., Beaudet, A.L., et al. (2009). Efficient, long-term hepatic gene transfer using clinically relevant HDAd doses by balloon occlusion catheter delivery in nonhuman primates. *Mol. Ther.* *17*, 327–333.
- Sendra, L., Miguel, A., Pérez-Enguix, D., Herrero, M.J., Montalvá, E., García-Gimeno, M.A., Noguera, I., Díaz, A., Pérez, J., Sanz, P., et al. (2016). Studying closed hydrodynamic models of "In Vivo" DNA perfusion in pig liver for gene therapy translation to humans. *PLoS One* *11*, e0163898.

17. Suda, T., Suda, K., and Liu, D. (2008). Computer-assisted hydrodynamic gene delivery. *Mol. Ther.* *16*, 1098–1104.
18. Chowdary, P., Shapiro, S., Makris, M., Evans, G., Boyce, S., Talks, K., Dolan, G., Reiss, U., Phillips, M., Riddell, A., et al. (2022). Phase 1–2 trial of AAVS3 gene therapy in patients with hemophilia B. *N. Engl. J. Med.* *387*, 237–247.
19. Nathwani, A.C., Tuddenham, E.G.D., Rangarajan, S., Rosales, C., McIntosh, J., Linch, D.C., Chowdary, P., Riddell, A., Pie, A.J., Harrington, C., et al. (2011). Adenovirus-associated virus vector-mediated gene transfer in hemophilia B. *N. Engl. J. Med.* *365*, 2357–2365.
20. Nathwani, A.C., Reiss, U.M., Tuddenham, E.G.D., Rosales, C., Chowdary, P., McIntosh, J., Della Peruta, M., Lheriteau, E., Patel, N., Raj, D., et al. (2014). Long-term safety and efficacy of factor IX gene therapy in hemophilia B. *N. Engl. J. Med.* *371*, 1994–2004.
21. Nathwani, A.C., Rosales, C., McIntosh, J., Rastegarlar, G., Nathwani, D., Raj, D., Nawathe, S., Waddington, S.N., Bronson, R., Jackson, S., et al. (2011). Long-term safety and efficacy following systemic administration of a self-complementary AAV vector encoding human FIX pseudotyped with serotype 5 and 8 capsid proteins. *Mol. Ther.* *19*, 876–885.
22. Brunetti-Pierri, N., Liou, A., Patel, P., Palmer, D., Grove, N., Finegold, M., Piccolo, P., Donnachie, E., Rice, K., Beaudet, A., et al. (2012). Balloon catheter delivery of helper-dependent adenoviral vector results in sustained, therapeutic hFIX expression in rhesus macaques. *Mol. Ther.* *20*, 1863–1870.
23. Song, S., Lyle, M.J., Noble-Vranish, M.L., Min-Tran, D.M., Harrang, J., Xiao, W., Unger, E.C., and Miao, C.H. (2022). Ultrasound-mediated gene delivery of factor VIII plasmids for hemophilia A gene therapy in mice. *Mol. Ther. Nucleic Acids* *27*, 916–926.
24. Yokoo, T., Kamimura, K., Suda, T., Kanefuji, T., Oda, M., Zhang, G., Liu, D., and Aoyagi, Y. (2013). Novel electric power-driven hydrodynamic injection system for gene delivery: safety and efficacy of human factor IX delivery in rats. *Gene Ther.* *20*, 816–823.
25. Cornu, T.I., Mussolino, C., and Cathomen, T. (2017). Refining strategies to translate genome editing to the clinic. *Nat. Med.* *23*, 415–423.
26. Wang, Q., Zhong, X., Li, Q., Su, J., Liu, Y., Mo, L., Deng, H., and Yang, Y. (2020). CRISPR-Cas9-Mediated *In Vivo* gene integration at the albumin locus recovers hemostasis in neonatal and adult hemophilia B mice. *Mol. Ther. Methods Clin. Dev.* *18*, 520–531.
27. Ohmori, T., Nagao, Y., Mizukami, H., Sakata, A., Muramatsu, S.I., Ozawa, K., Tominaga, S.I., Hanazono, Y., Nishimura, S., Nureki, O., et al. (2017). CRISPR/Cas9-mediated genome editing via postnatal administration of AAV vector cures haemophilia B mice. *Sci. Rep.* *7*, 4159.
28. Li, H., Haurigot, V., Doyon, Y., Li, T., Wong, S.Y., Bhagwat, A.S., Malani, N., Anguela, X.M., Sharma, R., Ivanciu, L., et al. (2011). *In vivo* genome editing restores haemostasis in a mouse model of haemophilia. *Nature* *475*, 217–221.
29. Singh, K., Evens, H., Nair, N., Rincón, M.Y., Sarcar, S., Samara-Kuko, E., Chuah, M.K., and VandenDriessche, T. (2018). Efficient *in vivo* liver-directed gene editing using CRISPR/Cas9. *Mol. Ther.* *26*, 1241–1254.
30. Nguyen, G.N., Everett, J.K., Kafle, S., Roche, A.M., Raymond, H.E., Leiby, J., Wood, C., Assenmacher, C.A., Merricks, E.P., Long, C.T., et al. (2021). A long-term study of AAV gene therapy in dogs with hemophilia A identifies clonal expansions of transduced liver cells. *Nat. Biotechnol.* *39*, 47–55.
31. Leebeek, F.W.G., and Miesbach, W. (2021). Gene therapy for hemophilia: a review on clinical benefit, limitations, and remaining issues. *Blood* *138*, 923–931.
32. George, L.A., Ragni, M.V., Rasko, J.E.J., Raffini, L.J., Samelson-Jones, B.J., Ozelo, M., Hazbon, M., Runowski, A.R., Wellman, J.A., Wachtel, K., et al. (2020). Long-term follow-up of the first in human intravascular delivery of AAV for gene transfer: AAV2-hFIX16 for severe hemophilia B. *Mol. Ther.* *28*, 2073–2082.
33. Pipe, S.W., Leebeek, F.W.G., Recht, M., Key, N.S., Castaman, G., Miesbach, W., Lattimore, S., Peerlinck, K., Van der Valk, P., Coppens, M., et al. (2023). Gene therapy with etranacogene dezaparvovec for hemophilia B. *N. Engl. J. Med.* *388*, 706–718.
34. Hurlbut, G.D., Ziegler, R.J., Nietupski, J.B., Foley, J.W., Woodworth, L.A., Meyers, E., Bercury, S.D., Pande, N.N., Souza, D.W., Bree, M.P., et al. (2010). Preexisting immu-
nity and low expression in primates highlight translational challenges for liver-directed AAV8-mediated gene therapy. *Mol. Ther.* *18*, 1983–1994.
35. Verdera, H.C., Kuranda, K., and Mingozzi, F. (2020). AAV vector immunogenicity in humans: a long journey to successful gene transfer. *Mol. Ther.* *28*, 723–746.
36. Mingozzi, F., and High, K.A. (2013). Immune responses to AAV vectors: overcoming barriers to successful gene therapy. *Blood* *122*, 23–36.
37. Manno, C.S., Pierce, G.F., Arruda, V.R., Glader, B., Ragni, M., Rasko, J.J., Ozelo, M.C., Hoots, K., Blatt, P., Konkle, B., et al. (2006). Successful transduction of liver in hemophilia by AAV-factor IX and limitations imposed by the host immune response. *Nat. Med.* *12*, 342–347.
38. Miesbach, W., Meijer, K., Coppens, M., Kampmann, P., Klamroth, R., Schutgens, R., Tangelder, M., Castaman, G., Schwäble, J., Bonig, H., et al. (2018). Gene therapy with adeno-associated virus vector 5-human factor IX in adults with hemophilia B. *Blood* *131*, 1022–1031.
39. Donsante, A., Miller, D.G., Li, Y., Vogler, C., Brunt, E.M., Russell, D.W., and Sands, M.S. (2007). AAV vector integration sites in mouse hepatocellular carcinoma. *Science* *317*, 477.
40. Suda, T., Gao, X., Stolz, D.B., and Liu, D. (2007). Structural impact of hydrodynamic injection on mouse liver. *Gene Ther.* *14*, 129–137.
41. Kanefuji, T., Yokoo, T., Suda, T., Abe, H., Kamimura, K., and Liu, D. (2014). Hemodynamics of a hydrodynamic injection. *Mol. Ther. Methods Clin. Dev.* *1*, 14029.
42. Colombo, P.C., Rastogi, S., Onat, D., Zacà, V., Gupta, R.C., Jorde, U.P., and Sabbah, H.N. (2009). Activation of endothelial cells in conduit veins of dogs with heart failure and veins of normal dogs after vascular stretch by acute volume loading. *J. Card. Fail.* *15*, 457–463.
43. Liakouli, V., Cipriani, P., Marrelli, A., Alvaro, S., Ruscitti, P., and Giacomelli, R. (2011). Angiogenic cytokines and growth factors in systemic sclerosis. *Autoimmun. Rev.* *10*, 590–594.
44. Hong, K.H., Ryu, J., and Han, K.H. (2005). Monocyte chemoattractant protein-1-induced angiogenesis is mediated by vascular endothelial growth factor-A. *Blood* *105*, 1405–1407.
45. Khan, A.A., Allemailem, K.S., Alhumaydhi, F.A., Gowder, S.J.T., and Rahmani, A.H. (2020). The biochemical and clinical perspectives of lactate dehydrogenase: an enzyme of active metabolism. *Endocr. Metab. Immune Disord. Drug Targets* *20*, 855–868.
46. Miao, C.H., Ye, X., and Thompson, A.R. (2003). High-level factor VIII gene expression *in vivo* achieved by nonviral liver-specific gene therapy vectors. *Hum. Gene Ther.* *14*, 1297–1305.
47. Miao, C.H., Ohashi, K., Patijn, G.A., Meuse, L., Ye, X., Thompson, A.R., and Kay, M.A. (2000). Inclusion of the hepatic locus control region, an intron, and untranslated region increases and stabilizes hepatic factor IX gene expression *in vivo* but not *in vitro*. *Mol. Ther.* *1*, 522–532.
48. Miao, C.H., Thompson, A.R., Loeb, K., and Ye, X. (2001). Long-term and therapeutic-level hepatic gene expression of human factor IX after naked plasmid transfer *in vivo*. *Mol. Ther.* *3*, 947–957.
49. Shibata, O., Kamimura, K., Tanaka, Y., Ogawa, K., Owaki, T., Oda, C., Morita, S., Kimura, A., Abe, H., Ikarashi, S., et al. (2022). Establishment of a pancreatic cancer animal model using the pancreas-targeted hydrodynamic gene delivery method. *Mol. Ther. Nucleic Acids* *28*, 342–352.
50. Zhang, J., Xu, L., Haskins, M.E., and Parker Ponder, K. (2004). Neonatal gene transfer with a retroviral vector results in tolerance to human factor IX in mice and dogs. *Blood* *103*, 143–151.
51. Vrekoussis, T., Chaniotis, V., Navrozoglou, I., Dousias, V., Pavlakis, K., Stathopoulos, E.N., and Zoras, O. (2009). Image analysis of breast cancer immunohistochemistry-stained sections using ImageJ: an RGB-based model. *Anticancer Res.* *29*, 4995–4998.
52. Ramesh, G., Santana-Gould, L., Inglis, F.M., England, J.D., and Philipp, M.T. (2013). The Lyme disease spirochete *Borrelia burgdorferi* induces inflammation and apoptosis in cells from dorsal root ganglia. *J. Neuroinflammation* *10*, 88.